Comparative Study of Medical-grade and Off-the-Person ECG Systems

Carlos Carreiras[1], André Lourenço[1,2], Hugo Plácido da Silva[1] and Ana Fred[1]
[1]*Instituto de Telecomunicações, Av. Rovisco Pais 1, Lisboa, Portugal*
[2]*Instituto Superior de Engenharia de Lisboa, R. Cons. Emídio Navarro 1, Lisboa, Portugal*

Keywords: Pervasive Electrocardiology, Off-the-Person ECG Sensor, Morphological Analysis.

Abstract: Simplified, off-the-person electrocardiogram (ECG) sensor designs enable the introduction into everyday life of continuous, and pervasive ECG acquisition paradigms. This significantly augments the potential of applications such as remote health monitoring, emotion assessment, and ECG biometrics, among others. We accomplish this by reducing the number of contact points to just two, making use of a groundless setting. Additionally, acquisition is made at the hand palms or fingers through dry electrodes. In this paper, we describe such a system, comparing it against a standard 12-lead, medical-grade ECG system. Our analysis is based on the morphological similarity between individual heartbeat waveforms, as well as the general similarity between the synchronized time series. We show that the ECG signal acquired at the hands with our sensor is highly correlated with lead I from the standard system.

1 INTRODUCTION

The measurement and recording of the electrical activity of the heart, commonly known as the electrocardiogram (ECG), has come a long way since its introduction at the end of the 19th century. The first systematic study of the electrical activity of the human heart was performed by Augustus Waller in 1887 (Besterman and Creese, 1979). He used a Lippmann capillary electrometer to measure the electrical potential between two surface electrodes placed on the front and back of the chest. This device consisted of a capillary tube partially filled with mercury and a solution of sulfuric acid. The electrodes were connected to either side of the tube; when an electric pulse arrives, the surface tension of the mercury is altered, allowing it to climb up a small distance in the capillary tube. Weller combined the use of the Lippmann electrometer with a light source, allowing him to project the oscillations of the mercury in the capillary onto a photographic plate; the plate moved with the help of a toy train, producing a real-time recording of the heartbeat.

A few years later, Willem Einthoven used a string galvanometer to significantly advance the knowledge about the electrical activity of the heart, naming the various deflections of the ECG (P, Q, R, S, T, and later U), standardizing the use of three limb leads (Einthoven's Triangle), and correlating numerous electrocardiographic features with cardiovascular disorders (Barold, 2003). The string galvanometer consisted of a long conductive filament; when subjected to a strong magnetic field, the fialment oscillates in proportion to the current traveling through it. This movement is then amplified and projected onto a moving photographic plate.

Fast forward to the present, the ECG has become a perfectly established and mainstream technique, providing vital information for the diagnosis and prevention of a wide array of cardiovascular disorders (Drew et al., 2004; Chung, 1996). Clinical practice relies mainly on the widespread short-term ($<$ 1 minute) 12-lead ECG for diagnosis, and, in selected cases, on Holter monitors ($\sim$ 24 hour assessment). Nevertheless, the outreach of ECG data acquisition and processing can still be significantly improved upon, in the context of a pervasive healthcare framework, with off-the-person ECG sensor designs. The goal of off-the-person approaches is not to replace existing data acquisition procedures, but to enhance and complement current practices with a simplified sensor setup that can be introduced, transparently to the subject, in multiple aspects of his everyday life. This enables a more comprehensive assessment of cardiovascular function, contributing to the development of preventive behaviors and methodologies. Also, it opens the door to many potential applications, such as continuous monitoring, non-intrusive emotion assess-

Carreiras C., Lourenço A., Plácido da Silva H. and Fred A..
Comparative Study of Medical-grade and Off-the-Person ECG Systems.
DOI: 10.5220/0004675501150120
In *Proceedings of the International Congress on Cardiovascular Technologies* (IWoPE-2013), pages 115-120
ISBN: 978-989-8565-78-5

ment (Haag et al., 2004; Medina, 2009) and ECG biometrics (Lourenço et al., 2011; Odinaka et al., 2012), among others.

In previous work by our team, we have proposed a simplified, off-the-person ECG sensor design targeted at data acquisition in a pervasive framework (Silva et al., 2011). In this paper, we compare the performance of this sensor against a medical-grade 12-lead standard ECG device, assessing the morphological and structural differences between both signals. The remainder of this paper is organized as follows: Section 2 provides an overview of our off-the-person sensor design, highlighting the main technical options, and details the acquisition setup; Section 3 describes the signal processing techniques employed, and the similarity measures used to compare the signals under study; finally, Section 4 outlines the main conclusions.

2 EXPERIMENTAL SETUP

With the goal of designing a non-intrusive, pervasive ECG sensor, we have been focusing our work on minimizing the number of electrical contact points with the subject's body, and eliminating the need for any gel or conductive paste in the electrode-skin interface. In this section, we present the general design guidelines adopted for the development of our off-the-person sensor, as well as the description of the signal acquisition setup used for the comparison of our sensor with a medical-grade ECG system.

2.1 Off-the-Person Sensor

Targeting the context of pervasive ECG acquisition, our sensor design uses only two dry electrodes, being based on the classical voltage potential differential principle. In particular, the sensor does not require the placement of a ground electrode, which is replaced by a reference voltage produced by the circuit (commonly known as a *virtual ground*).

According to the literature (Webster, 2009), typical physiological ECG signals range from 0.5 to 4 mV in amplitude, with a spectral content between 0.01 and 250 Hz. These small amplitudes require the use of high-quality, low-noise instrumentation and operational amplifiers, with high common-mode rejection at the input. The global gain of our system is set at 2000. However, given the use of dry electrodes and a groundless setting, our system is more prone to high-frequency noise. Therefore, the sensor incorporates a band-pass filter with a passing band between 0.5 and 40 Hz, simultaneously reducing the effect of the low-frequency respiratory modulation, as well as the powerline and high-frequency noise.

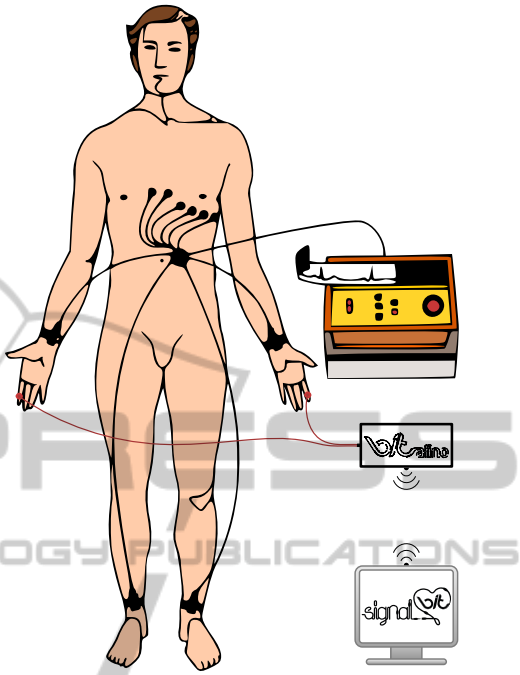

Figure 1: Schematic representation of the classical 12-lead ECG placement system, along with the placement of our off-the-person sensor approach, with the dry electrodes placed at the hands (drawings not to scale).

Figure 1 illustrates the typical 12-lead ECG system, as well as the placement of our off-the-person sensor, using two dry electrodes placed at the hands. Our ECG sensor is integrated into a broader signal acquisition hardware framework, the *BITalino* platform (Guerreiro et al., 2013), which wirelessly transmits the acquired ECG signal to a computing device. Note that, although our sensor was specifically designed for 1-lead measurements at the hand palms or fingers with virtual ground, it can also be used with a ground electrode, being capable of emulating any of the bipolar ECG leads (the Einthoven leads: I, II and III).

2.2 Acquisition and Preprocessing

We conducted experimental tests involving 11 volunteers (5 females and 6 males) in which simultaneous recordings were performed using a Philips PageWriter Trim series ECG device (hereinafter referred to as *Philips*), and our off-the-person sensor design (hereinafter referred to as *BITalino*) with data acquisition performed using the *SignalBIT* platform (Alves et al., 2013). The acquisitions were made on two sessions, separated by $\sim$ 1.5 months, but three of

the subjects only partook in one of the sessions (subjects S1, S3 and S6).

The *Philips* equipment was used in the standard 12-lead configuration (I-III, V1-V6, aVF, aVL, aVR), as shown in Figure 1, with conductive gel applied to each of the electrodes, which were placed on the subjects by an experienced technician. It acquires signal data at $500\,Hz$, with $16\,bit$ resolution, and storage is made in a proprietary file format. Our sensor was used in the virtual ground setting with dry Ag/AgCl electrodes, and the subjects were told to hold the electrodes at the hands. The *BITalino* device acquires signal data at $1000\,Hz$, with $10\,bit$ resolution, and storage is made in the open *StorageBIT* file format (Carreiras et al., 2013a). Given the fact that the *Philips* system records only 10 seconds of data for each run, we acquired three sequential runs, thus amounting to 30 seconds of data per subject per session.

The main application of our sensor has been to ECG biometrics (Lourenço et al., 2011; Silva et al., 2013; Carreiras et al., 2013b), reason for which both signals were filtered with a Finite Impulse Response (FIR) bandpass filter with a Hamming window of $300\,ms$, and cutoff frequencies of $5-20\,Hz$. These parameters were determined to be appropriate for this specific application (Lourenço et al., 2012).

Additionally, for the comparison measures we employ in this paper, it is necessary to have both signals with the same sample rate. Therefore, and given the characteristics of the filter just described, we downsampled the *BITalino* signal by a factor of 2, making it match the $500\,Hz$ sampling rate of the *Philips* device.

3 COMPARATIVE STUDY

We base our comparative study of the *BITalino* sensor and the *Philips* system on two major approaches: morphological and synchronized analyses. While the first approach focuses on the shape similarity between individual heartbeat waveforms, the second focuses on analyzing the correlation between the signals after a synchronization step, i.e. the correction of the time delay between the two independent data acquisition systems.

3.1 Morphological Analysis

In this paper, morphological analysis is understood to be the comparison of the shape similarity between individual heartbeat waveforms, as measured by a specified metric. This requires the use of a QRS detection algorithm, which enables the segmentation and extraction of the individual heartbeat waveforms from the ECG time series. For that purpose, we used the modified Engzee algorithm described in (Lourenço et al., 2012), which identifies the positions of the R peaks in the ECG. We then extract the signal segment corresponding to $200\,ms$ before and $400\,ms$ after each R peak, amounting to a total of $600\,ms$, which corresponds to the RR interval with a heart rate of $100\,bpm$ (see Figure 2). We applied this segmentation algorithm to the signals from both devices, collecting, from each subject, all the identified heartbeat waveforms across both sessions. Note that in the case of the *Philips* device, segmentation was performed using the signal from lead I, using it as reference for the other leads, i.e. the positions of the R peaks found using lead I were used to extract the individual heartbeats from the other leads.

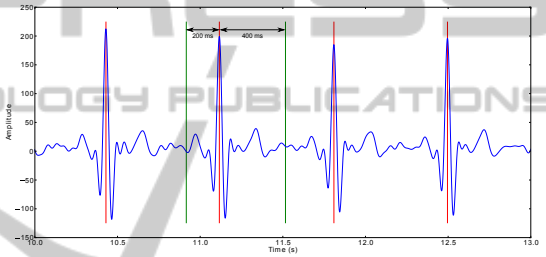

Figure 2: Example of the segmentation and heartbeat waveform extraction procedure; the positions of the R peaks are plotted in red vertical lines; the limits of one of the heartbeats are shown in green.

Figure 3 shows the heartbeat waveforms obtained for one of the subjects, comparing the *BITalino* heartbeats with each of the leads from the *Philips* system. We can observe that the most visually similar *Philips* lead to the *BITalino* heartbeats is lead I, as intended by the design of the sensor described in the previous section, with an almost complete overlap between the two. It is also possible to distinguish two groups of heartbeats in the Figure, identifiable, for example, by looking at the T waves. This is due to the fact that the Figure shows the heartbeats from both acquisition sessions, for which the subject happened to have different resting heart rates. As it is known (Simoons and Hugenholtz, 1975), the heart rate influences the relative position of the ECG waves, in particular the T wave.

For the quantitative analysis, given the use of different electrode types and gains between the *Philips* and *BITalino* devices, we adopted the cosine distance as similarity metric (Equation 1), which is bounded between 0 and 1, respectively representing complete similarity (vectors with same orientation) and complete dissimilarity (vectors at $\pi/2$).

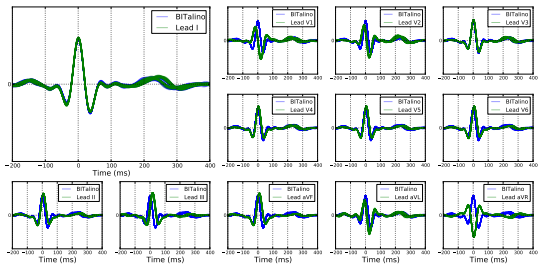

Figure 3: Segmented heartbeat waveforms obtained for subject S8 with both devices; the *BITalino* heartbeats are reproduced in each plot, comparing them with each of the leads from the *Philips* system.

$$D_{cos}(x_i,x_j) = 1 - \frac{\sum_{k=1}^{N} x_i[k]x_j[k]}{\sum_{k=1}^{N} x_i^2[k] \sum_{k=1}^{N} x_j^2[k]} \qquad (1)$$

We use this metric to compare, for each subject, the distance of the segmented heartbeat waveforms: a) within the *BITalino* sensor (*BIT vs BIT*); b) within lead I of the *Philips* system (*I vs I*); and c) of the *BITalino* device against the segmented heartbeat waveforms of each of the *Philips* leads (*BIT vs X*). Figure 4 shows the boxplots describing the general distribution characteristics, across all subjects, of the cosine distances obtained for each of the previously mentioned items. We can see that the most similar *Philips* lead to the *BITalino* sensor is lead I, as it presents the lowest median and narrowest Interquartile Range (IQR) of the compared leads. Additionally, these values are the most similar to the ones obtained in the *BIT vs BIT* and the *I vs I* cases. This reinforces, with quantitative information, the conclusion drawn earlier when comparing the heartbeat waveforms of one of the subjects. Also of note is the fact that the *BIT vs BIT* distribution appears to have a wider IQR when compared to that of the *I vs I* case, as well as two distinct groups of outliers. This suggests that the *BITalino* sensor is somewhat more sensitive to noise. To better analyze this question, we also show in Figure 5 the histograms of these two distributions, for all subjects. Indeed, the *BITalino* sensor produces distributions with higher means, with a slower decay as the distance increases. In two specific cases (subjects S6 and S9), the *BITalino* system originates some heartbeats with high dissimilarity to the others, arising from the existence of spurious, noisy heartbeats for these subjects (e.g. resulting from motion artifacts). Again, note that the two distribution modes observable in subject S8 result from different resting heart rates between the acquisition sessions.

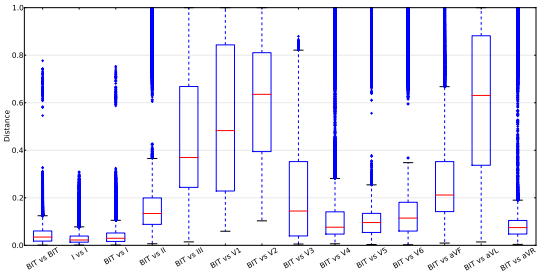

Figure 4: Boxplots, across all subjects, of the cosine distance of the *BITalino* heartbeats against the heartbeats of each of the *Philips* leads; the whiskers extend to the lowest and highest data points still within 1.5 times the Interquartile Range; crosses represent outliers.

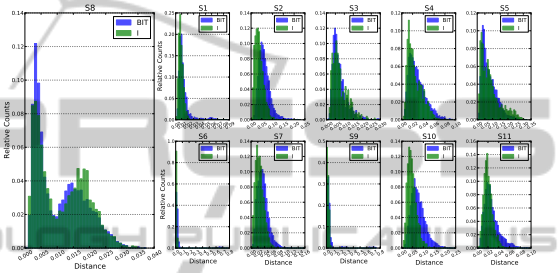

Figure 5: Histograms, for all subjects, of the cosine distance between the *BITalino* heartbeats (BIT), and between the heartbeats from lead I of the *Philips* system (I).

3.2 Synchronized Analysis

The synchronized analysis corresponds to the comparison of the two ECG sensor systems after the signals have been aligned in the time domain. We accomplish this by first normalizing the DC offset and amplitude of the signals, as shown in Equation 2, where the original signal $x[k]$ is subtracted of its mean μ, and divided by the total amplitude variation.

$$x_{norm}[k] = \frac{x[k] - \mu}{\max_k \{x[k]\} - \min_k \{x[k]\}} \qquad (2)$$

We then aligned the signals between corresponding *BITalino* and *Philips* runs by computing the time delay for which the cross-correlation between them (Equation 3) is maximum. Note that we use the lead I from the *Philips* system to determine the delay, given that we demonstrated in the previous section that this derivation is the same as the one used by the *BITalino* sensor.

$$d^* = \arg\max_{d \in \mathbb{Z}} \sum_{k=-\infty}^{+\infty} x[k]\, y[k+d] \qquad (3)$$

Figure 6 shows an example of the synchronized signals for one of the acquisition runs, where we can observe that there is an almost exact match between

the two signals. This is further validated by computing the Root Mean Square Error (RMSE), as defined in Equation 4.

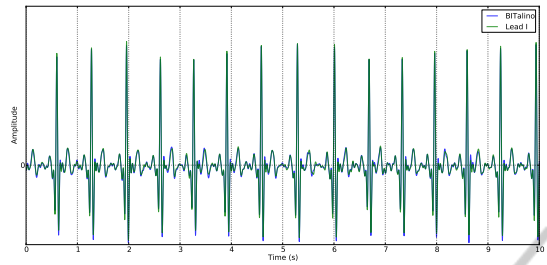

Figure 6: Synchronized *BITalino* and *Philips* lead I signals (subject S8); normalization using Equation 2.

$$RMSE(x,y) = \sqrt{\frac{\sum_{k=1}^{N}(x[k]-y[k])^2}{N}} \quad (4)$$

Figure 7 shows, for each subject, the averaged (across all runs) RMSE between the synchronized *BITalino* signal and each of the *Philips* leads. We can see that the error to lead I is indeed small, although we lack a reference with which to formulate stronger conclusions. It is also interesting to note that subject S10 exhibits a different pattern to that of the other subjects of the RMSE across the various leads. This arises due to the subject having a rotation of the heart axis, resulting in different projections onto the typical ECG derivations.

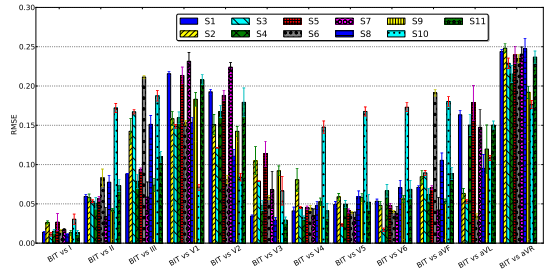

Figure 7: Root Mean Square Error between the *BITalino* and *Philips* lead I synchronized signals, for all subjects; values are the averages across all runs.

Finally, we use the cosine distance to compare the individual heartbeats of the synchronized signals, computing the distance between each *BITalino* heartbeat waveform and the corresponding aligned *Philips* heartbeat waveform. We show the results in Figure 8, where we can observe that the comparison against lead I exhibits a very small variability, and a median close to zero. This allows us to conclude that the *BITalino* and the *Philips* lead I signals are highly correlated.

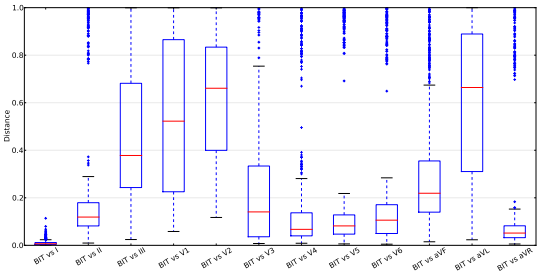

Figure 8: Boxplots, across all subjects, of the cosine distance of the synchronized *BITalino* heartbeats against the heartbeats of each of the *Philips* leads; the whiskers extend to the lowest and highest data points still within 1.5 times the Interquartile Range; crosses represent outliers.

4 CONCLUSIONS

In this paper we described a simplified ECG sensor design targeted at pervasive, off-the-person acquisition, comparing it with a standard 12-lead, medical-grade ECG system. Our analysis was based on the morphological similarities between individual heartbeat waveforms, and also on the general similarity between the synchronized time series.

The main conclusion of this paper is that the ECG signal acquired at the hands with our sensor is most similar to lead I from the standard system, showing a high degree of correlation between them. This result strongly encourages us to further investigate the off-the-person acquisition paradigm, especially for ECG biometrics. In this particular case, it is important, in order to develop a practical system, to have ECG acquisition setups that are non-intrusive and seamlessly integrate into everyday objects. In the future, we would like to compare the recognition accuracy of an ECG biometric system using our off-the-person sensor design, against the standard 12-lead ECG system.

ACKNOWLEDGEMENTS

This work was partially funded by Fundação para a Ciência e Tecnologia (FCT) under grants PTDC/EEI-SII/2312/2012, SFRH/BD/65248/2009 and SFRH/PROTEC/49512/2009, whose support the authors gratefully acknowledge.

REFERENCES

Alves, A. P., Silva, H., Lourenço, A., and Fred, A. (2013). SignalBIT A web-based platform for real-time biosig-

nal visualization and recording. In *Proc. of the 10th SIGMAP*.

Barold, S. S. (2003). Willem Einthoven and the birth of clinical electrocardiography a hundred years ago. *Cardiac electrophysiology review*, 7(1):99–104.

Besterman, E. and Creese, R. (1979). Waller–pioneer of electrocardiography. *Brit. Heart J.*, 42(1):61.

Carreiras, C., da Silva, H. P., Lourenço, A., and Fred, A. L. N. (2013a). StorageBIT: A Metadata-aware, Extensible, Semantic, and Hierarchical Database for Biosignals. In *Proc. of the 6th HEALTHINF*.

Carreiras, C., Lourenço, A., Silva, H., and Fred, A. L. N. (2013b). A Unifying Approach to ECG Biometric Recognition Using the Wavelet Transform. In *Proc. of the 10th ICIAR*.

Chung, E. K. (1996). *Pocket guide to ECG diagnosis*. Blackwell Science.

Drew, B. J., Califf, R. M., Funk, M., Kaufman, E. S., Krucoff, M. W., Laks, M. M., Macfarlane, P. W., Sommargren, C., Swiryn, S., and Van Hare, G. F. (2004). Practice standards for electrocardiographic monitoring in hospital settings. *Circulation*, 110(17):2721–2746.

Guerreiro, J., Martins, R., Silva, H., Lourenço, A., and Fred, A. L. N. (2013). BITalino: A Multimodal Platform for Physiological Computing. In *Proc. of the 10th ICINCO*.

Haag, A., Goronzy, S., Schaich, P., and Williams, J. (2004). Emotion recognition using bio-sensors: First steps towards an automatic system. In *Aff. Dial. Syst.*, pages 36–48. Springer.

Lourenço, A., Silva, H., and Fred, A. (2011). Unveiling the biometric potential of Finger-Based ECG signals. *Computational Intelligence and Neuroscience*, 2011.

Lourenço, A., Silva, H., Leite, P., Lourenço, R., and Fred, A. (2012). Real time electrocardiogram segmentation for finger based ECG biometric. In *Proc. of the 5th BIOSIGNALS*, pages 49–54.

Lourenço, A., Silva, H., and Fred, A. L. N. (2012). ECG-based biometrics: A real time classification approach. In *Proc. of the IEEE MLSP Workshop*.

Medina, L. (2009). Identification of stress states from ECG signals using unsupervised learning methods. Master's thesis, Universidade Técnica de Lisboa, Instituto Superior Técnico.

Odinaka, I., Lai, P.-H., Kaplan, A., O'Sullivan, J., Sirevaag, E., and Rohrbaugh, J. (2012). ECG biometric recognition: A comparative analysis. *IEEE Trans. Inf. Forensics Security*, 7(6):1812 –1824.

Silva, H., Lourenço, A., Lourenço, R., Leite, P., Coutinho, D., and Fred, A. (2011). Study and evaluation of a single differential sensor design based on electro-textile electrodes for ECG biometrics applications. In *Proc. IEEE Sensors Conf.*

Silva, H., Lourenço, A., Canento, F., and Fred, A. (2013). ECG Biometrics: Principles and Applications. In *Proc. of the 6th BIOSIGNALS*.

Simoons, M. and Hugenholtz, P. (1975). Gradual changes of ECG waveform during and after exercise in normal subjects. *Circulation*, 52(4):570–577.

Webster, J. G. (2009). *Medical Instrumentation Application and Design*. Wiley, 4th edition.